

Highly Efficient Platinum(II) Complexes Overcoming Pt-Pt Interactions and Their Applications in Organic Light-emitting Diodes

Keke Wan, Chen Lu, Nannan Cong, Kuo Lv, Zenghui Dai and Feng Li*

State Key laboratory of Supramolecular Structure and Materials, College of Chemistry Jilin University,
Qianjin Avenue 2699, Changchun 130012, P. R. China.

E-mail: lifeng01@jlu.edu.cn

Contents

1. Synthesis and Characterization	1
1.1. Synthesis.....	1
1.2. Characterization.....	2
1.2.1. ¹H-NMR spectra of ligands LA – LC	3
1.2.2. Ion trap gas chromatography-mass spectrometry of LA - LC ...	4
1.2.3. ¹H-NMR spectra of coordination complexes 1 – 3.....	5
1.2.4. MALDI-TOF mass spectra of Pt-1 – Pt-3.....	6
1.3. Structures.....	7
1.4. Thermogravimetric analysis	8
2. The photophysical properties of coordination complexes Pt-1 – Pt-3 ..	8
3. OLEDs Performances	10
3.1. CV curves	11
3.2. Chemical structures of TAPC, CBP and POT2T	11
4. References.....	11

1. Synthesis and Characterization

1.1. Synthesis

Synthesis of A 4-Trifluoromethyl-1,2-phenylenediamine (6 mmol, 1.057 mg), benzaldehyde (7.2 mmol, 0.7641 g), and Sodium Pyrosulfite ($\text{Na}_2\text{S}_2\text{O}_5$, 6 mmol, 1.141 g) were added to a 250 mL double mouth round bottom flask. Then, after removing the air by a vacuum pump and filling with the Argon for three times, the dry N,N-dimethylformamide 60 mL was poured into the bottom flask. The solution was continuously heated 8 hours with 110 °C. After cooling to the room temperature, the solution was pulled into the 500 mL aqua astricta and stirred for 2 hours. The filled white solid was dried under 50 °C for five hours and without further purifications.

Synthesis of B Being similar to the method of synthesizing **A**, **B** was synthesized that the 4-fluorobenzene-1,2-diamine (6 mmol, 0.757 mg) replaced the 4-Trifluoromethyl-1,2-phenylenediamine without further purifications.

Synthesis of C Being similar to the method of synthesizing **A**, **C** was synthesized that the 3,4-Diaminotoluene replaced the 4-fluoro-1,2-phenylenediamine (6 mmol, 0.733 mg) and the time of reaction was extended to 12 hours without further purifications.

Synthesis of LA A (2.14 mmol, 0.560 g), sodium hydroxide (2.58 g, 2 g mL⁻¹), tetrabutylammonium (2.56 mmol, 0.942 g), toluene 17 mL were added to a 100 mL. After removing the air and filling with the Argon, bromide benzyl bromide (3.21 mmol, 0.549 g) was followed under Argon conditions. The solution was continuously heated overnight with 110 °C. By the method of column chromatography, 0.63 g **LA** (1-benzyl-2-(3-(trifluoromethyl)phenyl)-1*H*-benzo[d]imidazole) was obtained with 84% yield. ¹H-NMR (500 MHz, CD₂Cl₂, 298 K, δ(ppm)): 7.95 (d, H, 2-ph-H), 7.74 (dd, 2H, 2-ph-H), 7.55 (m, 5H, ph-H); 7.37 (m, 2H, ph-H); 7.12 (d, 2H, 1-ph-H); 5.56 (s, 2H, CH₂-H).

Synthesis of LB Being similar to the method of synthesizing **LA**, **LB**(1-benzyl-2-(3-fluorophenyl)-1*H*-benzo[d]imidazole) was synthesized that the B (2.14 mmol, 0.447 g) replaced the A. As a result, 0.48 g **LB** was obtained with 48% yield. ¹H-NMR (500 MHz, CD₂Cl₂, 298 K, δ(ppm)): 7.73 (m, 2H, 2-ph-H), 7.53 (m, 4H, ph-H), 7.36 (m, 3H, ph-H); 7.19 (dd, 1H, ph-H); 7.12 (m, 2H, 1-ph-H); 7.03 (m, 1H, 1-ph-H); 5.50 (s, 2H, CH₂-H).

Synthesis of LC Being similar to the method of synthesizing **LA**, **LC** (1-benzyl-2-(m-tolyl)-1*H*-benzo[d]imidazole) was synthesized that the C replaced the A. As a result, 0.52 g **LC** was obtained with 81% yield. ¹H-NMR (500 MHz, CD₂Cl₂, 298 K, δ(ppm)):7.62 (m, 6H, 2-ph-H), 7.37 (m, 3H, ph-H), 7.06 (m, 4H, ph-H); 5.44 (d, 2H, CH₂-H); 2.29 (d, 0.5H, CH₃-H); 1.43 (m, 1.5H, CH₃-H); 0.95 (dt, 1H, CH₂-H).

Synthesis of Pt-1' Based on the reported method, the precursor coordination complexes **Pt-1'** were synthesized. ligands A (1 mmol, 0.352 g), K₂PtCl₄ (1 mmol, 0.415 g), 10 mL ultrapure water and 30 mL 2-ethoxyethanol were added to a 100 mL Schlenk flask. After removed the air and filed with the Argon, the mixture was heated to 80 °C for 24 hours. Then, cooled to the room temperature and poured into the ice water, the solid products were obtained. Without further purification, **Pt-1'** 0.72 g was obtained.

Synthesis of Pt-2' Being similar to the method of synthesizing **Pt-1'**, **Pt-2'** was synthesized that the (1 mmol, 0.302 g) replaced the **LA**. As a result, 0.55 g **Pt-2'** was obtained.

Synthesis of Pt-3' Being similar to the method of synthesizing **Pt-1'**, **Pt-3'** was synthesized that the **LC** (1 mmol, 0.298 g) instead of the **LA**. As a result, 0.39 g **Pt-3'** was obtained.

Synthesis of Pt-1 Pt-1' (0.2 mmol, 0.232 g), natrium carbonicum (Na_2CO_3 , 0.62 mmol, 0.067 g) and 12 mL 2-ethoxyethanol was added to a 100 mL Schlenk flask. After removing the air and filed with the Argon,

2,2,6,6-Tetramethyl-3,5-heptanedione (0.62 mmol, 0.100 g) was added to the solution under the Argon conditions. Then, the mixture was continuously heated 115 °C for 24 hours. After purified by the method of column chromatography, the green powders of 120 mg were collected with 39% yield. Anal. In the refrigerator at -28 °C, methanol slowly volatilized to the ethyl acetate solution of **Pt-1**, which was placed for about 6 days to obtain single crystals. Calcd. for $C_{32}H_{33}F_3N_2O_2Pt$: C, 52.67; H, 4.56; N, 3.84%; Found: C, 52.90; H, 4.569; N, 3.23%. 1H -NMR (500 MHz, DMSO- d_6 , 298 K, δ (ppm)): 8.88 (s, 1H, ph-H), 8.08 (d, 1H, ph-H), 7.77 (d, 1H, ph-H), 7.65 (d, 1H, ph-H), 7.59 (d, 1H, ph-H), 7.35 (d, 2H, ph-H), 7.29 (d, 1H, ph-H), 7.17 (m, 3H, ph-H), 7.02 (d, 1H, CH-H), 6.15 (s, 2H, CH₂-H), 1.32 (s, 9H, CH₃-H), 1.27 (s, 9H, CH₃-H). MALDI-TOF mass (m/z): [**Pt-1**], and [**Pt-1**-(ph-CH₂)] calcd.: 729.21, and 638.16, respectively; found.: [(**Pt-1**)-2H⁺] 727.34, and [(**Pt-1**-(ph-CH₂))-H⁺] 637.58.

Synthesis of Pt-2-H₂O Similar to that of **Pt-1**, instead, **Pt-2'** (0.2 mmol, 0.213 g) was used and the product was obtained as green powders (83 mg) after the purification by the method of column chromatography with 29% yield. The single crystal of **Pt-2** was collected by by volatilizing a mixture of dichloromethane and petroleum ether at room temperature for 1 day. Anal. Calcd. for $C_{32}H_{35}F_3N_2O_3Pt$: C, 53.37; H, 5.06; N, 4.02%; Found: C, 53.01; H, 4.800; N, 3.53%. 1H -NMR (500 MHz, DMSO- d_6 , 298 K, δ (ppm)): 8.48 (m, 0.5H, ph-H), 8.28 (m, 0.5H, ph-H), 7.86 (t, 1H, ph-H), 7.62 (d, 1H, ph-H), 7.53 (m, 1H, ph-H), 7.33 (m, 5H, ph-H), 7.16 (d, 2H, ph-H), 6.99 (d, 2H, pPh-H), 6.07 (d, 2H, CH₂-H), 5.92 (d, 1H, CH-H), 1.32 (d, 9H, CH₃-H), 1.25 (s, 9H, CH₃-H). MALDI-TOF mass (m/z): [**Pt-2**], and [**Pt-2**-(ph-CH₂)] calcd.: 679.22, and 588.16, respectively; found.: 679.81, and 587.72.

Synthesis of Pt-3 Similar to that of **Pt-1**, instead, **Pt-3'** (0.2 mmol, 0.211 g) was used and the product was obtained as green powders (100 mg) after the purification by the method of column chromatography with 35% yield. Single crystal of the complex **Pt-3** were obtained after 5 days by the same way method of growing single crystal **Pt-1**. Anal. Calcd. for $C_{32}H_{33}F_3N_2O_2Pt$: C, 56.88; H, 5.37; N, 4.15%; Found: C, 57.45; H, 5.547; N, 3.66%. 1H -NMR (500 MHz, DMSO- d_6 , 298 K, δ (ppm)): 8.39 (d, 1H, ph-H), 7.65 (dd, 2H, ph-H), 7.51 (dd, 1H, ph-H), 7.30 (m, 4H, ph-H), 7.12 (m, 2H, ph-H), 6.97 (dd, 1H, ph-H), 6.03 (d, 2H, CH₂-H), 5.91 (d, 1H, CH-H), 2.47 (d, 3H, CH₃-H), 1.33 (d, 9H, CH₃-H), 1.26 (d, 9H, CH₃-H). MALDI-TOF mass (m/z): [**Pt-3**], and [**Pt-3**-(ph-CH₂)] calcd.: 675.24, and 584.19, respectively; found.: 675.10, and 583.91.

1.2. Characterization

Elemental analysis (C, H and N) was performed on a Elementar Vario micro cube elemental analyzer. Thermogravimetric analysis (TGA) was investigated on a TA INSTRUMENTS Q500 instrument with a heating rate of 10 °C·min⁻¹ in Nitrogen atmosphere. Ultraviolet-visible (UV-vis) absorption spectra were collected on a Shimadzu UV-2550 spectrophotometer. Fluorescence spectra were collected on a RF-6000. PLQEs of thin-films and solutions were collected on a FS920 fluorescence/phosphorescence spectrophotometer and integrating sphere. Tetrabutylammonia hexafluorophosphate and dry acetonitrile are the electrolyte and solvent. The sweep speed is 100 mV·s⁻¹. The oxidation and reduction points pair, ferrocene cation and ferrocene, was the internal standard. The 1H -NMR spectra were recorded at 298 K with a Bruker AVANCZ 500 spectrometer, using deuterated dimethyl sulfoxide (DMSO) as solvent and tetramethyl silane (TMS) as standard. Electrospray Ionization Mass Spectrometry (ESI-MS) was performed on Agilent1290 - Bruker micrOTOF QII.

1.2.1. $^1\text{H-NMR}$ spectra of ligands LA – LC

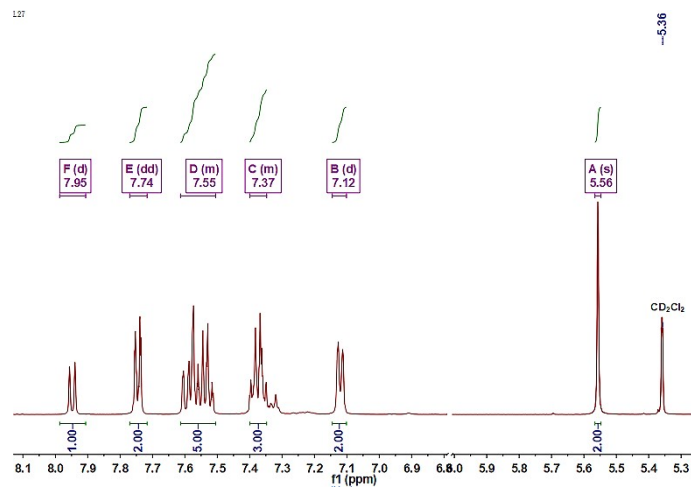


Fig. S1 The $^1\text{H-NMR}$ spectrum of LA for 500 MHz in CD_2Cl_2 in 298 K.

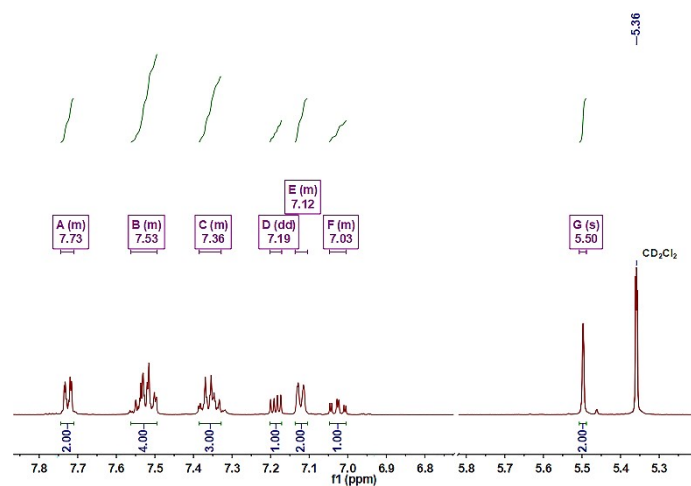


Fig. S2 The $^1\text{H-NMR}$ spectrum of LB for 500 MHz in CD_2Cl_2 in 298 K.

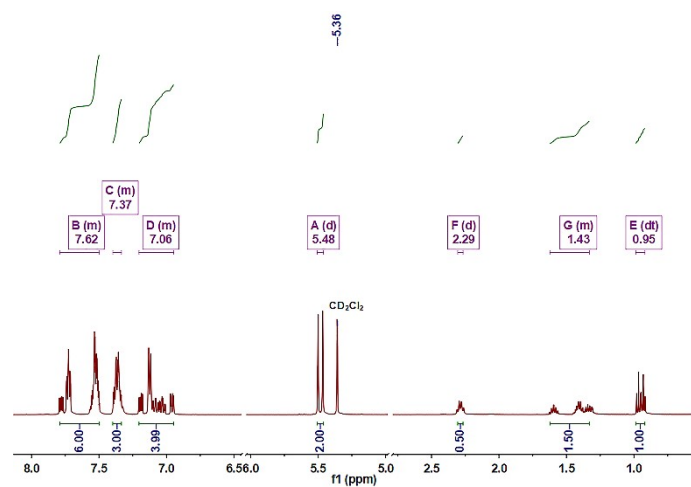


Fig. S3 The $^1\text{H-NMR}$ spectrum of LC for 500 MHz in CD_2Cl_2 in 298 K.

1.2.2. Ion trap gas chromatography-mass spectrometry of LA - LC

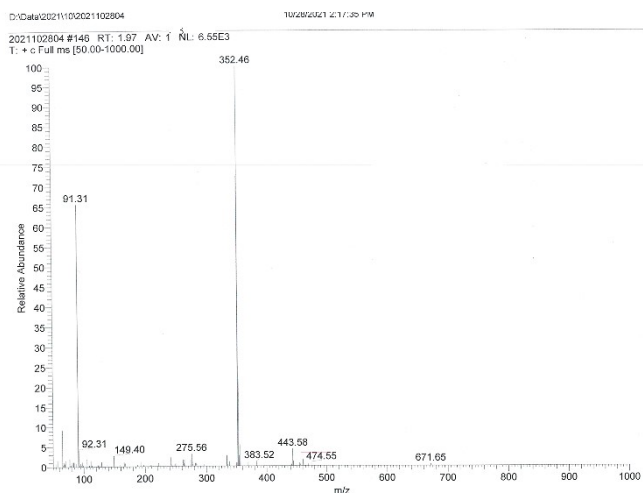


Fig. S4 Ion trap gas chromatography-mass spectrometry of LA.

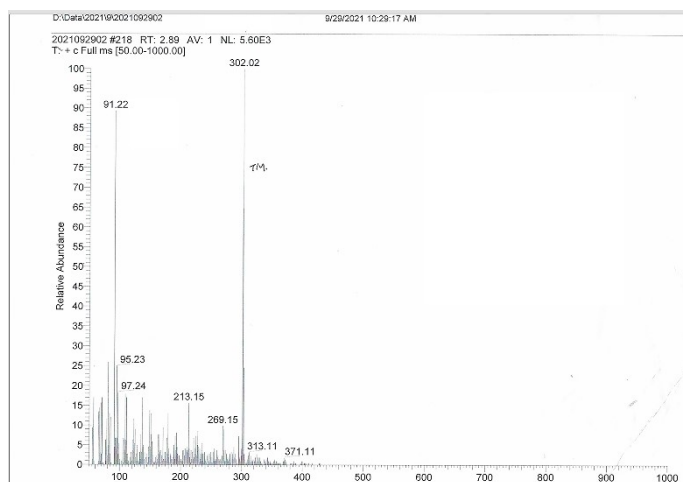


Fig. S5 Ion trap gas chromatography-mass spectrometry of LB.

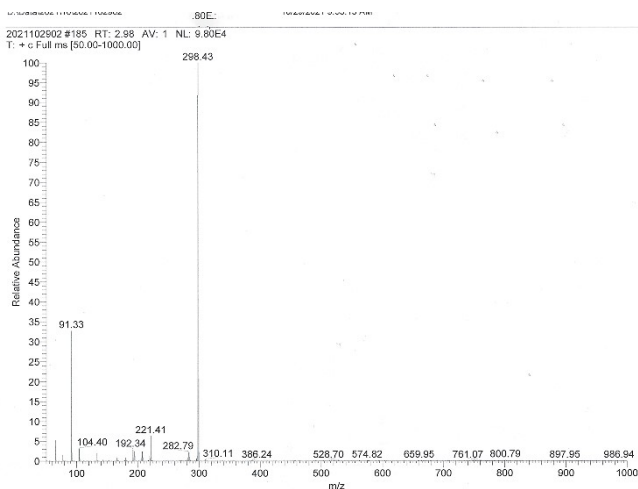


Fig. S6 Ion trap gas chromatography-mass spectrometry of LC.

1.2.3. $^1\text{H-NMR}$ spectra of coordination complexes 1 – 3

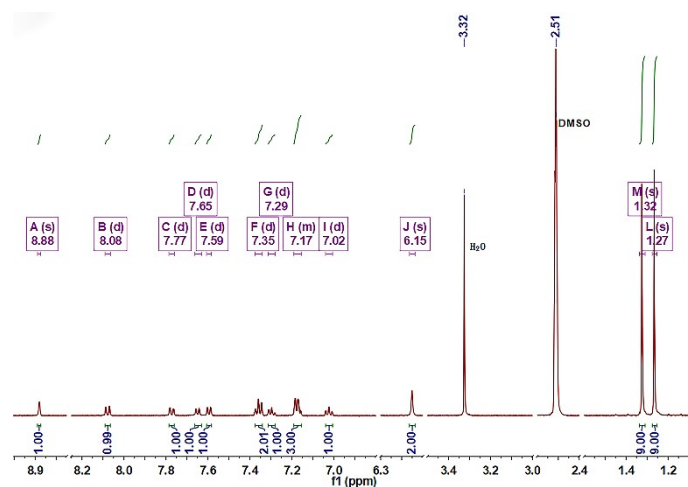


Fig. S7 The $^1\text{H-NMR}$ spectrum of Pt-1 for 500 MHz in DMSO-d_6 in 298 K.

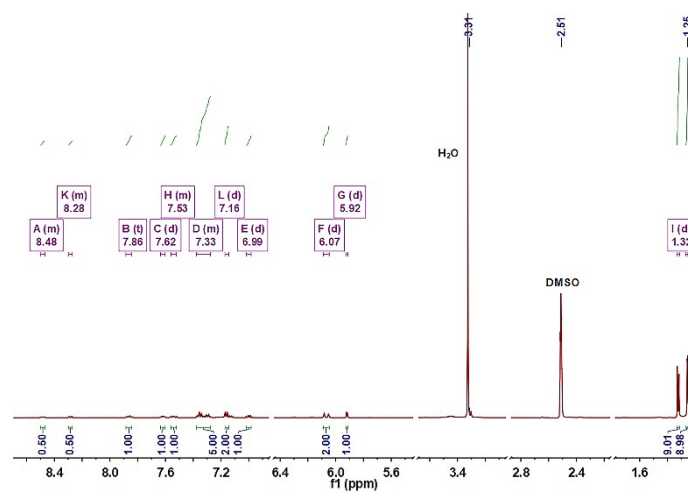


Fig. S8 The $^1\text{H-NMR}$ spectrum of Pt-2 for 500 MHz in DMSO-d_6 in 298 K.

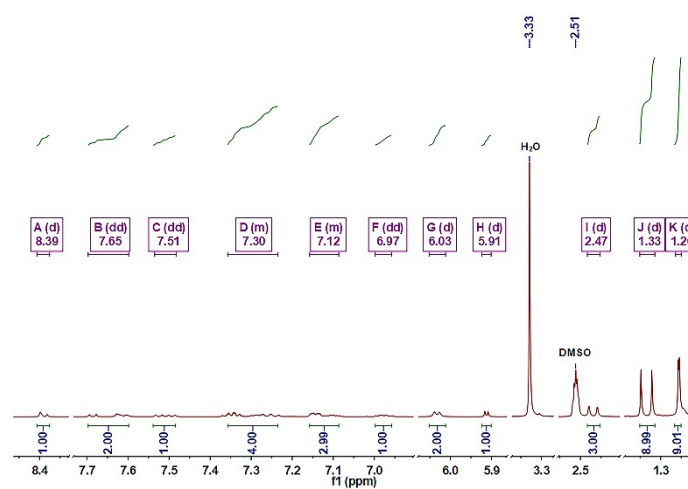


Fig. S9 The $^1\text{H-NMR}$ spectrum of Pt-3 for 500 MHz in DMSO-d_6 in 298 K.

1.2.4. MALDI-TOF mass spectra of Pt-1 – Pt-3

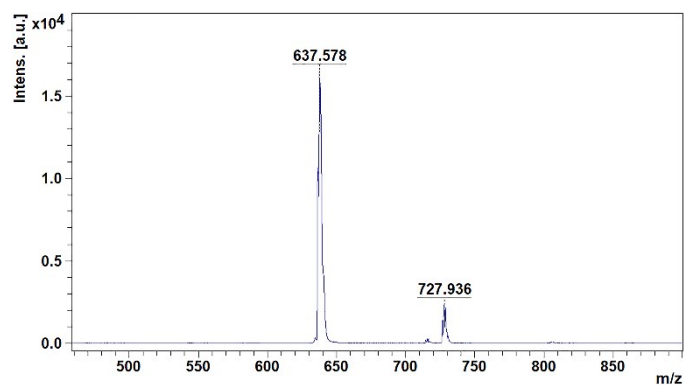


Fig. S10 MALDI-TOF mass spectra of the coordination complex **Pt-1**.

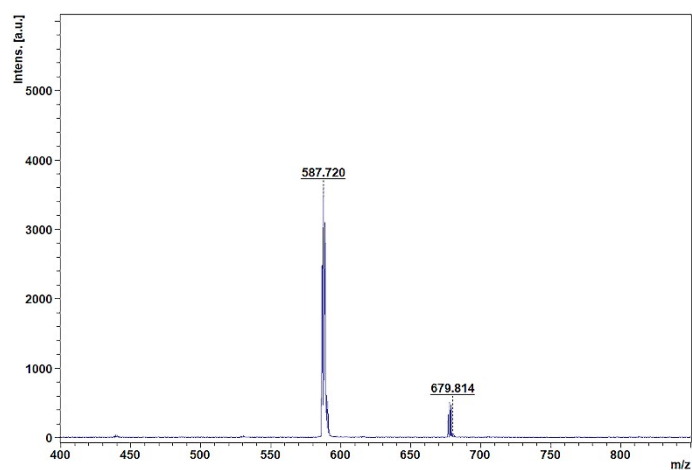


Fig. S11 MALDI-TOF mass spectra of the coordination complex **Pt-2**.

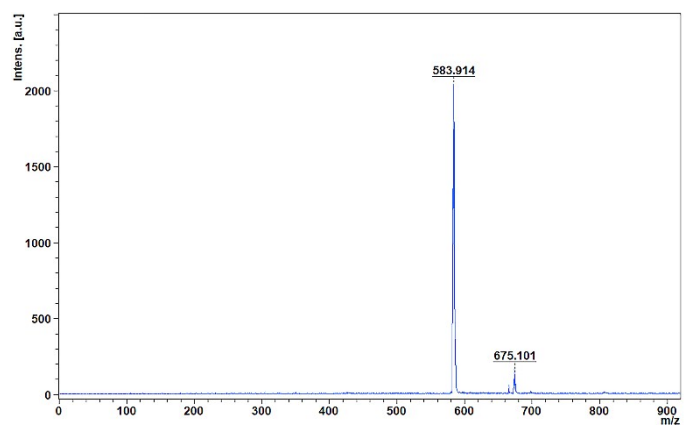


Fig. S12 MALDI-TOF mass spectra of the coordination complex **Pt-3**.

1.3. Structures

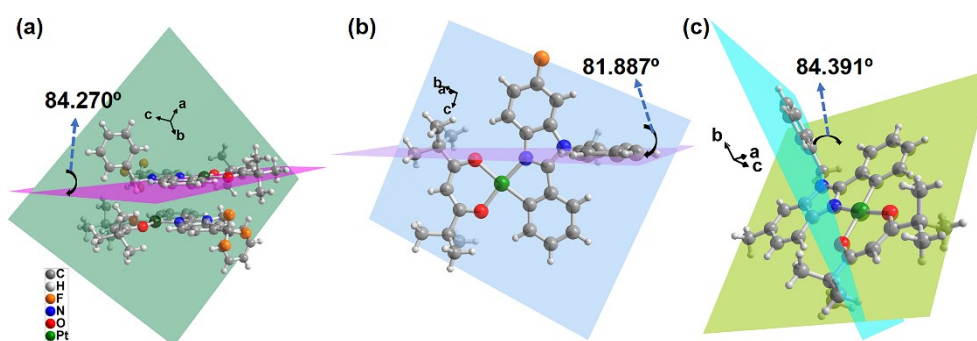


Fig. S13 The asymmetric units and dihedral angles of three complexes, **Pt-1** – **Pt-3**.

Table S1 Crystallographic data of all the title complexes.

	Pt-1	Pt-2	Pt-3
Formula	C ₃₂ H ₃₃ F ₃ N ₂ O ₂ Pt	C ₃₁ H ₃₃ FN ₂ O ₂ Pt	C ₃₂ H ₃₆ N ₂ O ₂ Pt
M	729.69	679.68	675.72
T (K)	100.00	100.00	100.00
Crystal system	Triclinic	Monoclinic	Triclinic
Space group	<i>P</i> ₁	<i>C</i> _{2/c}	<i>P</i> ₁
a (Å)	11.0394(4)	18.6880(7)	11.0801(6)
b (Å)	11.5345(5)	12.8330(7)	11.4438(6)
c (Å)	13.3691(5)	24.3979(10)	13.3443(7)
α (°)	111.180(2)	90	113.058(2)
β (°)	94.980(2)	100.718(2)	94.169(2)
γ (°)	111.237(2)	90	110.653(2)
V (Å³)	1432.39(10)	5749.1(4)	1412.45(13)
Z	2	8	2
D_c (g mL⁻¹)	1.692	1.571	1.589
μ (mm⁻¹)	4.949	4.917	4.998
Reflections collected	54546	137733	30029
Unique reflections	6571	6612	4981
R_{int}	0.0414	0.0481	0.0655
Goof	1.074	1.041	1.069
R₁, I > 2σ(I)	0.0216	0.0682	0.0721
wR₂, all data	0.0493	0.1765	0.1691

1.4. Thermogravimetric analysis

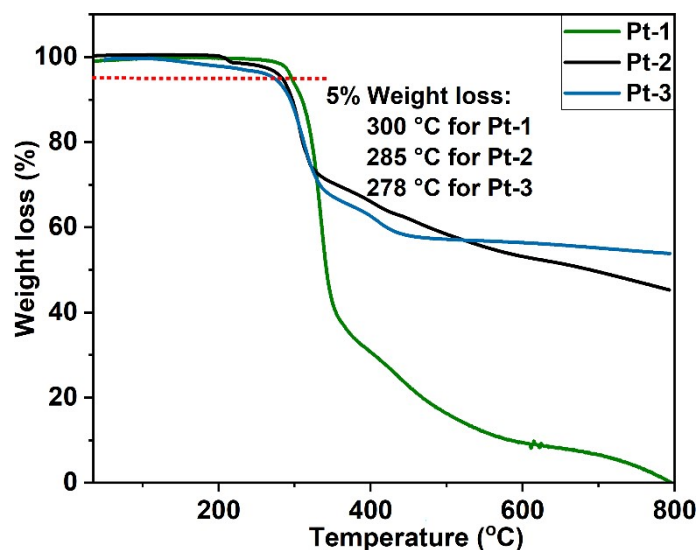


Fig. S14 The TGA curves of Pt-1, Pt-2, and Pt-3.

2. The photophysical properties of coordination complexes Pt-1 – Pt-3

The radiative transition constant (k_r) and the non-radiative transition constant (k_{nr}) are calculated as the follows ¹:

$$\phi_{fl} = \frac{k_r}{k_r + k_{nr}} \quad (1)$$

$$\tau = \frac{1}{k_r + k_{nr}} \quad (2)$$

Where ϕ_{fl} and τ are PLQE and Lifetimes, respectively.

Table S2 The photophysical properties of coordination complexes Pt-1 – Pt-3 in films and solutions.

CPs	States	λ_{abs}	λ_{ex}	λ_{em}	T^c	ϕ_{fl}	Stokes shift	k_r	k_{nr}
		nm			μs	%	nm	$\times 10^5 s^{-1}$	
Pt-1	In PMMA ^a	310,371,408	406	488,522	5.56	~99 ^d	80	1.78	0.018
	In DCM ^b	313,375,408	408	491,527	4.01	77 ^d	83	1.92	0.57
	Pure film	315,375,412	411	490,524	6.38	~99 ^e	77	1.55	0.016
Pt-2	In PMMA ^a	315,368,405	403	490,524	5.07	~99 ^d	87	1.95	0.02
	In DCM ^b	315,367,402	404	494,530	5.23	75 ^d	92	1.43	0.48
	Pure film	317,371,405	406	499,535	7.46	97 ^e	92	1.30	0.04
Pt-3	In PMMA ^a	317,366,403	402	492,428	5.55	79 ^d	90	1.42	0.38
	In DCM ^b	317,365,400	401	497,533	6.06	46 ^d	96	0.76	0.89
	Pure film	319,369,404	402	500,536	7.07	83 ^e	95	1.17	0.24

^a The coordination complexes were doped in the PMMA with the weight concentration of 1wt.%; ^b The solutions of coordination complexes in DCM removed oxygen with the concentration of 1×10^{-5} mol mL⁻¹; ^c the optical maser of 375 nm, the detected emission wavelengths based on the shortest emission peaks in the measurements; ^d $\lambda_{ex} = 310$ nm); ^e $\lambda_{ex} = 416$ nm.

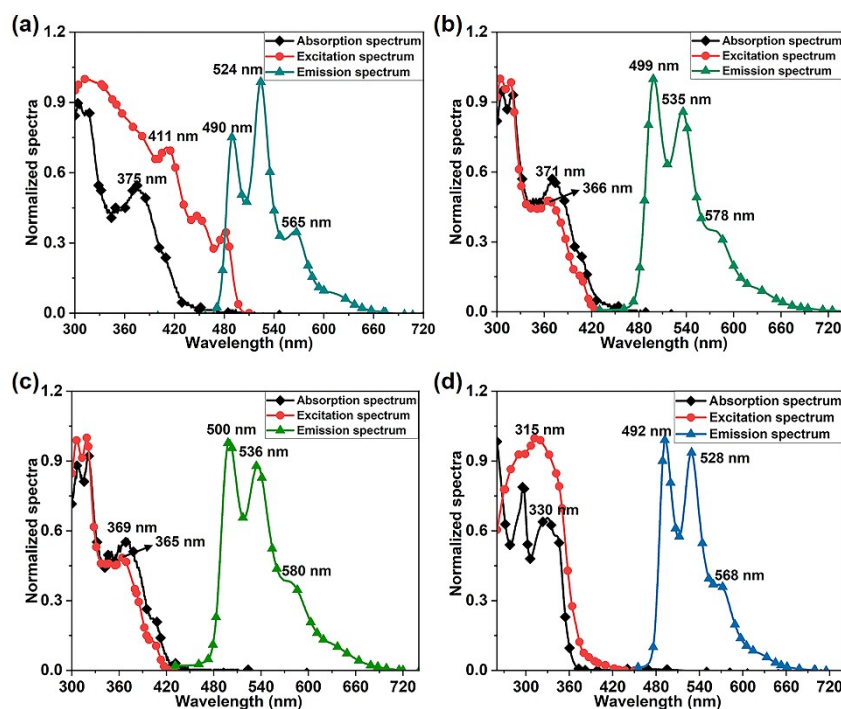


Fig. S15 The normalized spectra of deposit pure films: (a) absorption, excitation (λ_{em} : 524 nm) and emission spectra (λ_{ex} : 375 nm) of **Pt-1**; (b) absorption, excitation (λ_{em} : 535 nm) and emission spectra (λ_{ex} : 371 nm) of **Pt-2**; (c) absorption, excitation (λ_{em} : 536 nm) and emission spectra (λ_{ex} : 369 nm) of **Pt-3**; and (d) The normalized absorption, excitation (λ_{em} : 528 nm) and emission spectra (λ_{ex} : 310 nm) of coordination complexes **Pt-1** doped in **CBP** with the weight concentration of 8wt.%.

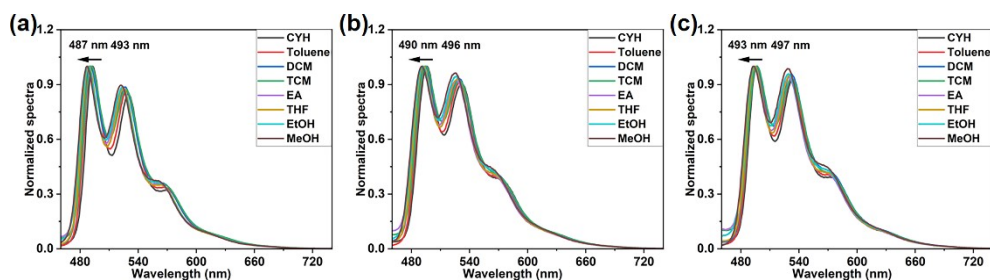


Fig. S16 PL of three complexes in different polarity of solvents: (a) **Pt-1**; (b) **Pt-2**; and (c) **Pt-3**. (CYH: cyclohexane; DCM: dichloromethane; TCM: trichloromethane; EA: ethyl acetate; THF: tetrahydrofuran; EtOH: ethyl alcohol; MeOH: methyl alcohol).

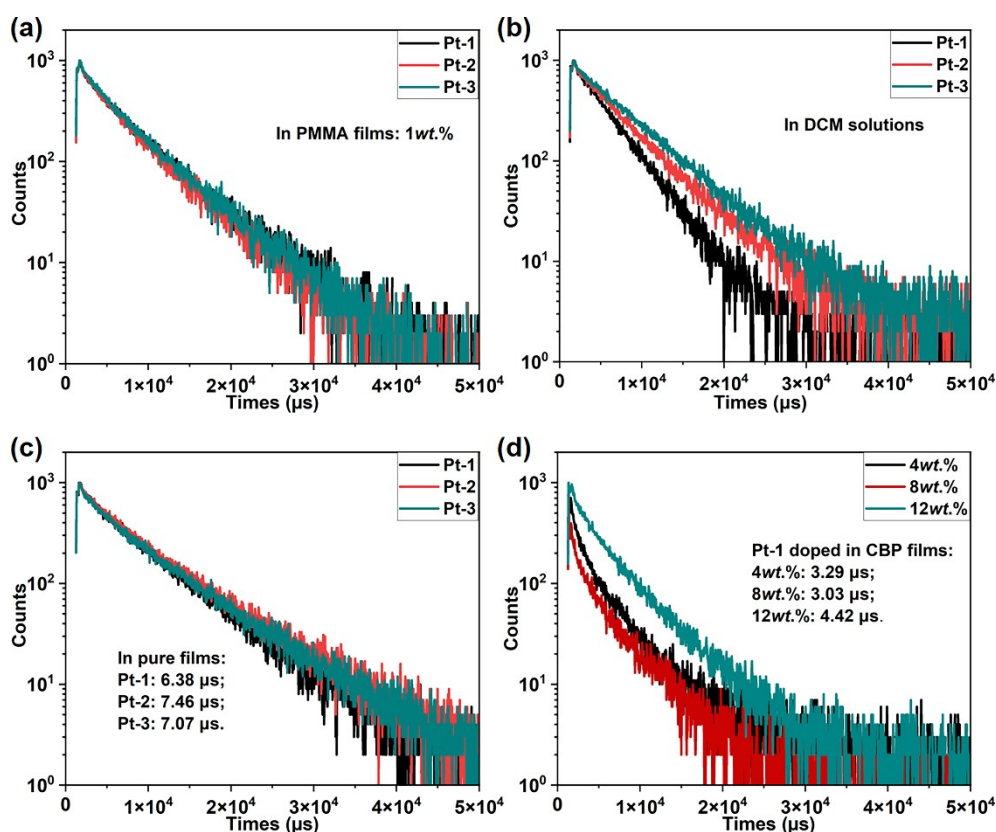


Fig. S17 The PL decay characteristics of **Pt-1**, **Pt-2**, and **Pt-3** in different states. (a) Doped in PMMA with the weight concentration of 1wt.%; (b) Dissolved in DCM solutions removed oxygen with the concentration of $1 \times 10^{-5} \text{ mol L}^{-1}$; (c) In pure films; and (d) **Pt-1** doped in CBP with the weight concentration of 4wt.%, 8wt.%, and 12wt.%.

3. OLEDs Performances

Pre-purchased indium tin oxide (ITO) glass substrates were obtained and subjected to a thorough cleaning process. Subsequently, after dried using nitrogen gas, they were exposed to UV irradiation for a duration of 30 minutes. The treated substrates were then transferred to a vacuum deposition system with a pressure maintained between 2×10^{-6} to 6×10^{-6} Pa. In this system, a layer of MoO_3 was deposited at a controlled rate of 0.1 \AA s^{-1} , while all organic layers were deposited at rates ranging from $0.3 - 0.4 \text{ \AA s}^{-1}$. The emitting layers were deposited at rates ranging from 0.2 \AA s^{-1} . The deposition temperatures are $179 - 197 \text{ }^\circ\text{C}$ for **Pt-1**, $170 - 172 \text{ }^\circ\text{C}$ for **Pt-2**, and $167 - 171 \text{ }^\circ\text{C}$ for **Pt-3**, respectively. The cathode LiF layer was evaporated at rates of less than 0.1 \AA s^{-1} . The Al metal layer was evaporated at rates of $0.8 - 0.9 \text{ \AA s}^{-1}$. All electrical testing and optical measurements were performed under air conditions. The electroluminescence spectra, as well as the measurements of luminance-voltage-current density ($L-V-C$), and external quantum efficiency (EQE), were conducted using a computer-controlled Keithley 2400 source meter. Additionally, absolute EQE measurements were performed using the C9920-12 system equipped with a photonic multichannel analyzer (PR-655). Cyclic Voltammetry (CV) data were measured on a CH Instruments CHI660E electrochemistry workstation with a three-electrode structure that glassy carbon electrode, platinum electrode, and Fe/Fe^+ electrode was regard as working electrode, counter electrode, and reference electrode, respectively.

3.1. CV curves

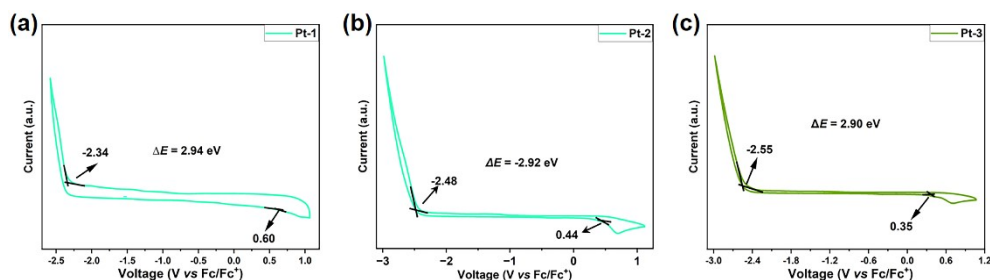


Fig. S18 CV curves of coordination complexes **Pt-1 – Pt-3** in dry DCM (electrolytes: tetrabutylammonium hexafluorophosphate).

Formula (3) – (4) Based on the data deduced from the cyclic voltammetry curves, HOMO and LUMO energy levels for the coordination complex are calculated as the following formula ²:

$$\text{LUMO} = [-(E_{\text{re}} - E_{1/2, \text{Ferrocene}}) + (-4.8)] \text{ eV} \quad (3)$$

$$\text{HOMO} = [-(E_{\text{ex}} - E_{1/2, \text{Ferrocene}}) + (-4.8)] \text{ eV} \quad (4)$$

$$\Delta E_{\text{LUMO-HOMO}} = (\text{LUMO} - \text{HOMO}) \text{ eV} \quad (5)$$

Table S3 Calculated (Cal.) and Experimental (Exp.) HOMO and LUMO energy levels, and energy gaps ($\Delta E_{\text{LUMO-HOMO}}$) for **Pt-1 – Pt-3**.

	HOMO (eV)		LUMO (eV)		$\Delta E_{\text{LUMO-HOMO}}$ (eV)	
	Cal.	Exp.	Cal.	Exp.	Cal.	Exp.
Pt-1	-5.48	-5.40	-1.93	-2.46	3.55	2.94
Pt-2	-5.27	-5.24	-1.73	-2.32	3.54	2.92
Pt-3	-5.14	-5.15	-1.63	-2.25	3.51	2.90

3.2. Chemical structures of TAPC, CBP and POT2T

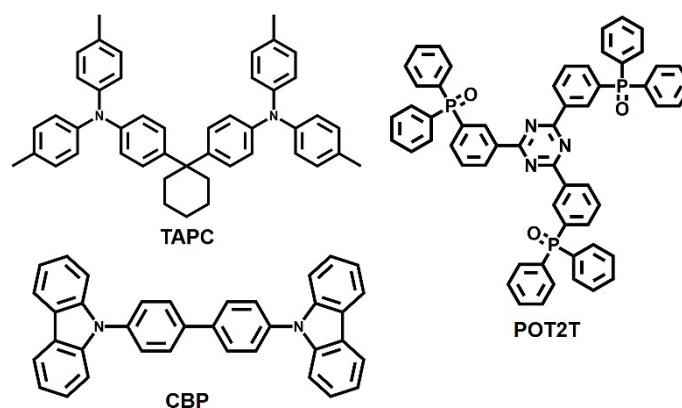


Fig. S19 Chemical structures of TAPC, CBP and POT2T.

4. References

1. A. Abdurahman, Y. X. Chen, X. Ai, O. Ablikim, Y. Gao, S. Z. Dong, B. Li, B. Yang, M. Zhang, F. Li, *J. Mater. Chem. C*, 2018, **42**, 11248-11254.
2. Q. Wu, D. Deng, J. Zhang, W. Zou, Y. Yang, Z. Wang, H. Li, R. Zhou, K. Lu, Z. Wei, *Sci. Chin. Chem.* 2019, **7**, 837-844.